An unorthodox sensory adaptation site in the *E. coli* serine chemoreceptor

Xue-Sheng Han and John S. Parkinson*

Biology Department

University of Utah

Salt Lake City, Utah 84112

Running title: E502: An unorthodox Tsr sensory adaptation site

*Corresponding author:

Mailing address: University of Utah, 257 South 1400 East, Salt Lake City, UT 84112

Phone: (801) 581-7639

FAX: (801) 581-4668

E-mail: parkinson@biology.utah.edu

Abbreviations:

MCP, methyl-accepting chemotaxis protein;

CW, clockwise; CCW, counter-clockwise;

MH, methylation helix;

IPTG, isopropyl β-D-thio-galactopyranoside

SDS-PAGE, sodium dodecyl sulfate-containing polyacrylamide gel electrophoresis

UU IR Author Manuscript

ABSTRACT

The serine chemoreceptor of *E. coli* contains four canonical methylation sites for sensory adaptation that lie near inter-subunit helix interfaces of the Tsr homodimer. An unexplored fifth methylation site, E502, lies at an intra-subunit helix interface, closest to the HAMP domain that controls input-output signaling in methyl-accepting chemotaxis proteins. We analyzed, with *in vivo* FRET kinase assays, the serine thresholds and response cooperativities of Tsr receptors with different mutationally imposed modifications at sites 1-4 and/or at site 5. Tsr variants carrying E or Q at residue 502 in combination with unmodifiable D and N replacements at adaptation sites 1-4, underwent both methylation and demethylation/deamidation, although detection of the latter modifications required elevated intracellular levels of CheB. These Tsr variants could not mediate a chemotactic response to serine spatial gradients, demonstrating that adaptational modifications at E502 alone are not sufficient for Tsr function. Moreover, E502 is not critical for Tsr function because only two amino acid replacements at this residue abrogated serine chemotaxis: Tsr-E502P had extreme kinase-off output; Tsr-E502I had extreme kinase-on output. These large threshold shifts are probably due to the unique HAMP-proximal location of methylation site 5. However, a methylation-mimicking glutamine at any Tsr modification site raised the serine response threshold, suggesting that all sites influence signaling by the same general mechanism, presumably through changes in packing stability of the methylation helix bundle. These findings are consistent with control of input-output signaling in Tsr through dynamic interplay of the structural stabilities of the HAMP and methylation bundles.

keywords: chemotaxis | dynamic-bundle model | methylation | deamidation

UU IR Author Manuscript

INTRODUCTION

Motile bacteria detect and follow gradients of attractant and repellent chemicals through chemotaxis signaling pathways (recent reviews: 1, 2, 3). The well-studied chemotaxis machinery of *E. coli* employs chemoreceptors known as methyl-accepting chemotaxis proteins (MCPs) to regulate the autophosphorylation activity of a cytoplasmic histidine kinase, CheA. A small cytoplasmic protein, CheW, couples CheA to receptor control. Ternary receptor signaling complexes form arrays at the cell poles that produce large changes in CheA activity in response to small changes in chemoeffector concentration. CheA, in turn, donates its phosphoryl groups to two cytoplasmic response regulators, CheY and CheB, to control, respectively, rotation of the cell's flagellar motors and a sensory adaptation process. Phosphorylation of CheY promotes clockwise (CW) motor rotation; phosphorylation of CheB augments its receptor-modifying enzymatic activities, demethylation or deamidation of specific MCP residues. Another cytoplasmic enzyme, CheR, is responsible for methylating receptor modification sites. The interplay of CheR and CheB activities regulates receptor methylation state to offset signaling responses to ambient chemoeffector levels, thereby adjusting sensitivity and extending detection range of the receptor array.

E. coli has four homodimeric, transmembrane MCPs (Fig. 1A) that detect various attractant compounds: Tsr (serine), Tar (aspartate and maltose), Tap (dipeptides and pyrimidines), and Trg (ribose and galactose). A fifth MCP-related receptor, Aer, has no periplasmic domain, but monitors cellular redox status through a cytoplasmic FAD-binding domain to mediate aerotactic behavior. All five of these MCP family receptors have highly similar cytoplasmic domains that form ternary signaling complexes with CheA and CheW. The Aer signaling domain contains no methylation sites and its mechanism of sensory adaptation remains unclear. In contrast, the other MCPs contain four canonical methylation sites per subunit. Each site resides in a 9-residue primary

structure motif ([A/S]-X-X-E-[**E/Q**]-X-[A/S/T]-A-[A/S/T]) thought to represent the consensus substrate site for CheB and CheR action (Fig. 1A) (4, 5). Both glutamate (E) and glutamine (Q) at the target residue (bold in the consensus) can serve as sites for adaptational modifications. CheB irreversibly deamidates Q's to E's; CheR methylates E's, forming glutamyl-methyl esters (Em); CheB demethylates Em sites by hydrolysis back to E. These four canonical sites are always the second residue of an E-E or E-Q pair and reside on the solvent-exposed faces of the cytoplasmic methylation helices (MH) where they most likely influence inter-subunit interactions in the four-helix MH bundle through electrostatic effects: Methylation should enhance MH packing stability; demethylation and deamidation should reduce MH packing stability (6, 7).

The serine receptor Tsr contains a fifth methylation site, E502, that does not conform to the consensus motif (Fig. 1A) (8). It is the first of an E-E pair and resides in a more buried location near the intra-subunit packing interface of the MH bundle (Fig. 1). Moreover, of the five Tsr methylation sites, E502 lies closest to the HAMP domain, which mediates input-output signaling transactions in chemoreceptors through its structural interplay with the MH bundle (9). These unique features could mean that E502 plays a different signaling role than do the canonical Tsr methylation sites. To explore that possibility, we constructed a series of mutant receptors with amino acid replacements at Tsr methylation sites and measured their methylation, demethylation, and deamidation properties and their serine dose-response signaling behaviors. Our results show that Tsr site 5 influences receptor signaling in the same way as do sites 1-4, but it has a much more potent effect on stimulus sensitivity, most likely owing to its proximity to the HAMP domain. These findings provide additional insights into the mechanisms of input-output signaling and sensory adaptation control in MCP molecules.

UU IR Author Manuscript

MATERIALS AND METHODS

Bacterial strains. Strains used in this study were isogenic derivatives of *E. coli* K-12 strain RP437 (10). Their designations and relevant genotypes were: UU1250 [*Δaer-1 Δtsr-7028 Δ(tar-tap)5201 Δtrg-100*] (11); UU2610 [*Δaer-1 Δ(tar-cheB)4346 Δtsr-5547 Δtrg-4543*] (12); UU2611[*Δaer-1 Δ(tar-cheR)4283 Δtsr-5547 Δtrg-4543*] (12); UU2612 [*Δaer-1 Δ(tar-tap)4530 Δtsr-5547 Δtrg-4543*] (12); UU2632 [*Δaer-1 Δ(tar-tap)4530 Δ(cheB)4345 Δtsr-5547 Δtrg-4543*] (12); UU2567 [*Δ(tar-cheZ)4211 Δ(tsr)-5547 Δ(aer)-1 Δtrg-4543*] (R.Z. Lai and J.S. Parkinson, manuscript in preparation); UU2697 [*Δ(cheY-cheZ)1215 Δ(cheB)4345 Δ(tar-tap)4530 Δtsr-5547 Δaer-1 Δtrg-4543*] (R.Z. Lai and J.S. Parkinson, manuscript in preparation); UU2699 [*Δ(cheY-cheZ)1215 Δ(tar-cheR)4283 Δtsr-5547 Δaer-1 Δtrg-4543*] (R.Z. Lai and J.S. Parkinson, manuscript in preparation); UU2700 [*Δ(cheY-cheZ)1215 Δ(tar-tap)4530 Δtsr-5547 Δaer-1 Δtrg-4543*] (R.Z. Lai and J.S. Parkinson, manuscript in preparation).

CheR/CheB phenotype notation. A shorthand notation is used throughout to indicate strain phenotypes with respect to the CheR (R^-, R^+) and CheB (B^-, B^+) proteins.

Plasmids. Plasmids used in the study were: pKG116, a derivative of pACYC184 (13) that confers chloramphenicol resistance and has a sodium salicylate-inducible expression/cloning site (14); pPA114, a relative of pKG116 that carries wild-type *tsr* under salicylate control (11); pRZ30, a derivative of pKG116 that carries *cheY-YFP* and *cheZ-CFP* fusions under salicylate control (R.Z. Lai and J.S. Parkinson, manuscript in preparation); pPA827, a derivative of pKG116 that carries wild-type *cheB* under salicylate control; pRR48, a derivative of pBR322 (15) that confers ampicillin resistance and has an expression/cloning site with a *tac* promoter and an ideal (perfectly palindromic) *lac* operator under the control of a plasmid-encoded *lacI* repressor, inducible by IPTG (16); pRR53, a derivative of pRR48 that carries wild-type *tsr* under IPTG control (16); and pVS88, a plasmid that carries *cheY-YFP* and *cheZ-CFP* fusions under IPTG control (17).

Chemotaxis assays. Host strains carrying *tsr* plasmids were assessed for chemotactic ability on tryptone or minimal glycerol plus serine soft agar plates (18) containing the appropriate antibiotics (ampicillin [50 μg/ml] or chloramphenicol [12.5 μg/ml]) and inducers (100 μM IPTG or 0.6 μM sodium salicylate). Tryptone plates were incubated at 30-32.5°C for 7-10 h or at 24°C for 15-20 h. Minimal plates were incubated at 30-32.5°C for 15-20 h.

Mutant construction. Mutations in the *tsr* gene of plasmids pPA114 or pRR53 were generated by QuikChange PCR mutagenesis, using either degenerate-codon or site-specific primers, as previously described (11). QuikChange products were introduced into UU1250 by $CaCl_2$ transformation and tested for the ability to support Tsr function on tryptone and minimal serine soft agar plates. Candidate plasmids were verified by sequencing the entire *tsr* coding region.

Expression levels and modification patterns of mutant Tsr proteins. Cells harboring pRR53 derivatives were grown in tryptone broth containing 50 μg/ml ampicillin and 100 μM IPTG; cells harboring pPA114 derivatives were grown in tryptone broth containing 12.5 μg/ml chloramphenicol and 0.6 μM sodium salicylate. Strain UU2610 (R^- B^-) was used for measuring expression levels of mutant proteins to avoid receptor molecules in multiple modification states. Strains UU2611(R^- B^+), UU2632 (R^+ B^-), and UU2612 (R^+ B^+) were used to assess the CheR and CheB substrate properties of mutant Tsr proteins. Cells were grown at 30°C to mid-exponential phase, and 1-ml samples were pelleted by centrifugation, washed twice with KEP (10 mM K-PO_4, 0.1 mM K-EDTA, pH 7.0), and lysed by boiling in sample buffer (19). Tsr bands were resolved by electrophoresis in 11% polyacrylamide gels containing sodium dodecyl sulfate and visualized by immunoblotting with a polyclonal rabbit antiserum raised against Tsr residues 290-470 (20). Gel band intensities were quantified with ImageJ software (*http://imagej.nih.gov/ij*).

Flagellar rotation assays. Flagellar rotation patterns of plasmid-containing cells were analyzed by antibody tethering as described previously (21). Cells were classified

UU IR Author Manuscript

into five rotation patterns and the fraction of CW rotation time for a population of tethered cells was computed by a weighted sum of these rotation classes, as described (11).

***In vivo* FRET CheA kinase assay.** The experimental system, cell sample chamber, stimulus protocol, and data analysis closely followed the hardware, software, and methods described by Sourjik *et al.* (17). Cells containing a FRET reporter plasmid (pRZ30 or pVS88) and a compatible *tsr* expression plasmid (pRR53 or pPA114 derivative) were grown to mid-exponential phase in tryptone broth, washed, attached to a round coverslip with polylysine, and mounted in a flow cell (22). The flow cell and all motility buffer test solutions [KEP containing 10 mM Na lactate, 100 μM methionine, and various concentrations of serine] were maintained at 30°C throughout each experiment. Cells were illuminated at the CFP excitation wavelength and light emission detected at the CFP (FRET donor) and YFP (FRET acceptor) wavelengths with photomultipliers. The ratio of YFP to CFP photon counts accurately reflects CheA kinase activity and changes in response to serine stimuli (23, 24). Fractional changes in kinase activity versus applied serine concentrations were fitted to a multi-site Hill equation, yielding two parameter values: $K_{1/2}$, the attractant concentration that inhibits 50% of the kinase activity; and the Hill coefficient, reflecting the extent of cooperativity of the response (17, 25).

Protein modeling and structural display. Structure images were prepared with MacPyMOL software (*http://www.pymol.org*). Atomic coordinates for the modeled Tsr methylation helix bundle were obtained from Professor Sung-Hou Kim (UC-Berkeley).

UU IR Author Manuscript

RESULTS

Mutational survey of Tsr-E502. To determine whether residue E502 is critical for Tsr function, we constructed derivatives of *tsr* expression plasmid pPA114 that encoded Tsr proteins with all possible amino acid replacements at the 502 position. On tryptone soft agar plates at an optimal inducer concentration of 0.6 μM sodium salicylate, the parental pPA114 plasmid confers robust serine chemotaxis to host strain UU1250, which carries deletions of all five *E. coli* MCP family genes (*tsr, tar, trg, tap* and *aer*) (11). All but two of the resulting E502 amino acid replacement mutant proteins (hereafter designated Tsr-E502*) conferred at least 50% of the wild-type colony size to the receptor-less host on tryptone soft agar (Fig. 2). This finding indicates that Tsr function tolerates a variety of amino acids at residue 502. However, subsequent chemotaxis tests on minimal soft agar plates containing 2.5, 20, or 100 μM serine showed that five of the functional Tsr mutants had elevated serine-sensing thresholds (Fig. 2). Overall, 12 Tsr-E502 amino acid replacements (R, A, T, L, C, W, F, S, V, Y, N, H) supported chemotaxis at 2.5 μM serine, as did wild-type (wt) Tsr; four (K, D, G, Q) produced chemotaxis at 20 μM serine; one (M) showed function at 100 μM serine; and two (I, P) could not mediate a chemotactic response at any serine concentration tested, including on tryptone medium, which contains ~670 μM serine (26).

SDS-PAGE analysis of Tsr-E502* proteins. The E502* mutants with impaired Tsr function might make a misfolded or unstable protein. To test this possibility, we measured the steady-state intracellular levels of all plasmid-expressed E502* proteins in the receptor-less host strain UU2610, which lacks the sensory adaptation enzymes, CheR and CheB (R^- B^-). Tsr subunits synthesized in this host strain lack adaptational modifications and, therefore, migrate as a single band on SDS-PAGE (11). Nearly all of the E502* proteins, including six of the seven impaired-function mutants (D, G, Q, M, I, P), had intracellular levels of 50% or more of the wild type (Fig. 2, gray bars).

Moreover, the mutant protein with the lowest expression level (E502N, 31% of Tsr-wt) had nearly full function (76% of Tsr-wt). We conclude that the E502* proteins have essentially normal expression levels and intracellular stabilities and that even those with functional defects probably have near-native structures.

Adaptational modifications can shift the SDS-PAGE mobility of MCP subunits: Methylated (or Q-bearing) forms migrate faster than do demethylated and deamidated (*i.e.*, E-bearing) forms. The mechanistic basis for those effects is unknown, but one possibility is that Tsr subunits retain residual secondary structures in SDS that influence electrophoretic mobility. Remarkably, every E502* mutant protein exhibited a different SDS-PAGE mobility than the wild-type protein (Fig. 2; Fig. S1). Tsr-E502P and Tsr-E502D migrated slower; all other mutant forms, regardless of their functional properties or side-chain chemical character, migrated faster than Tsr-wt. We consider implications of this phenomenon in the Discussion.

Measurement and interpretation of mutant Tsr signaling patterns. To assess the signaling properties of mutant Tsr receptors, we adopted a FRET-based kinase assay, developed by Sourjik and Berg (23), to follow *in vivo* Tsr control of CheA activity in response to serine stimuli. This assay measures interaction of YFP-tagged phospho-CheY (the FRET acceptor) and its CFP-tagged phosphatase CheZ (the FRET donor). The FRET signal reflects the receptor-coupled autophosphorylation activity of CheA, the rate-limiting step in CheY phosphorylation. The FRET dose-response data were fitted to a multi-site Hill equation to obtain a $K_{1/2}$ value, the attractant concentration that inhibits 50% of CheA activity, and a Hill coefficient, which reflects the extent of response cooperativity.

We interpret shifts in the serine response sensitivity of Tsr mutants in terms of a two-state signaling model in which receptor ternary complexes can adopt CheA-activating (kinase-on [ON] or CW) and CheA-deactivating (kinase-off [OFF] or CCW) output states. Accordingly, a cell's overall kinase activity and stimulus sensitivity reflect the proportions of receptor signaling complexes in the ON and OFF states. The OFF

state is assumed to have higher affinity for attractant ligands than does the ON state. Thus, chemoattractants elicit CCW flagellar responses by driving receptor signaling complexes to the OFF state. According to this two-state view, mutant receptors that show enhanced serine sensitivity (*i.e.*, lower $K_{1/2}$ values than the wild-type) should have equilibrium shifts toward the OFF state ("OFF-biased"). Conversely, mutant receptors with reduced serine sensitivity (*i.e.*, elevated $K_{1/2}$ values) should have equilibrium shifts toward the ON state ("ON-biased").

Signaling effects of adaptational modifications at E502. In the context of a two-state model, the sensory adaptation system shifts receptor signaling complexes to the ON or OFF states to cancel ligand-induced responses. CheR-mediated methylation at sites 1-4 favors the ON state; CheB-mediated demethylation or deamidation at sites 1-4 drives receptors toward the OFF state (1). To determine whether adaptational modifications at Tsr-E502 produce output effects similar to those at sites 1-4, we constructed a series of variant receptors with different combinations of E and Q residues at sites 1-5 and measured their serine thresholds and response cooperativities with *in vivo* FRET kinase assays. E residues represent the unmethylated state, whereas Q residues are closest in structure to glutamyl-methyl-esters and approximate the signaling effects of the methylated state (27). Mutant *tsr* plasmids were tested in a $CheR^-$ $CheB^-$ strain (UU2567) to preclude modification of the Q and E residues by the sensory adaptation system. The dose-response parameters are summarized in Table S1; representative curves are shown in Fig. 3A; and the relationship between number of Q sites and serine sensitivity is presented in Fig. 3B. These experiments showed, consistent with previous *in vivo* (24) and *in vitro* (27, 28) studies, that at sites 1-4 each Q residue progressively shifts Tsr to a higher serine threshold, *i.e.*, toward the ON state. A glutamine at site 5 also elevated the serine response threshold, suggesting that methylation at E502 affects Tsr output in the same way as does methylation at sites 1-4 (Fig. 3B). However, a Q at site 5 produced a much larger threshold increase than did a single Q at any other site (Fig. 3B). For example, a single Q at site 1, 2, 3, or 4

UU IR Author Manuscript

produced $K_{1/2}$ values ranging from ~2 μM (EEEQE) to ~5 μM (QEEEE) (Table S1), whereas the EEEEQ receptor had a $K_{1/2}$ value of ~100 μM (Table S1), substantially higher than even wild-type Tsr (QEQEE; $K_{1/2}$ ~17 μM), which has glutamines at both sites 1 and 3 (Fig. 3). These results imply that methylation at E502 produces a much larger shift toward the ON state than does methylation at sites 1-4.

To determine whether Tsr methylation site 5 alone could support serine chemotaxis, we used combinations of D and N replacements at sites 1-4 to approximate the signaling properties of the wild-type E and Q residues at those positions. Aspartate and asparagine closely resemble glutamate and glutamine, respectively, except that their side-chains are one methyl group shorter. Neither D nor N is an effective substrate for CheR and CheB modification reactions (see below). FRET kinase assays in the $R^- B^-$ strain showed that Tsr variants with combinations of D and N residues at sites 1-4 had signaling properties similar to their E and Q counterparts (Fig. 4; Table S2). For example, Tsr-NDDDE (Fig. 4) and Tsr-QEEEE (Fig. 3A) had comparable serine sensitivities; Tsr-NDNDE and wild-type Tsr (QEQEE) had similar sensitivities (Fig. 4; Table S2). Despite these normal dose-response behaviors in FRET assays, all Tsr variants with combinations of D and N residues at sites 1-4 failed to support serine chemotaxis of an $R^+ B^+$ strain (UU2612) on tryptone or minimal serine soft agar plates (Table S2). These findings indicate that E502 alone cannot support full Tsr function in cells that contain the sensory adaptation enzymes. Either Tsr residue E502 cannot undergo reversible methylation-demethylation reactions or those modifications are not sufficient for tracking spatial serine gradients.

CheR-dependent methylation of Tsr-E502. CheR promotes methylation of Tsr residue E502 (8), but how extensive and reversible that modification might be *in vivo* remain open issues. To look for *in vivo* methylation at site 5, we examined the SDS-PAGE band patterns of Tsr-DDDDE and Tsr-NDNDE molecules expressed in strains with different combinations of the CheR and CheB enzymes (Fig. 5). In hosts lacking CheR function ($R^- B^-$; $R^- B^+$), both receptors migrated as a single species, whereas in

hosts containing CheR (R^+ B^-; R^+ B^+), Tsr-DDDDE and Tsr-NDNDE subunits migrated as two species, the faster of which was unique to the hosts that had CheR function (Fig. 5A). These results suggest that residue E502 in both receptors can undergo CheR-mediated methylation. To determine whether that CheR-dependent modification required a glutamate residue at site 5, we compared the band profiles of Tsr-NDNDE with Tsr-NDNDD in the R^+ hosts (Fig. 5B). The subunits bearing the E502D replacement exhibited only one band, demonstrating that an aspartate residue could not support the modification. These findings indicate, consistent with a prior study of Tar methylation sites (29), that D residues at any of the Tsr modification sites are poor substrates for CheR-mediated methylation. Moreover, it appears that an N residue, at least at Tsr sites 1 and 3, is refractory to deamidation by physiological levels of CheB (Fig. 5A). We conclude, consistent with the original study of Rice and Dahlquist (8), that Tsr-E502 is subject to CheR-mediated methylation *in vivo*.

CheB-dependent deamidation of Tsr-E502. A glutamine at Tsr methylation site 1 or 3 can undergo *in vivo* CheB-mediated deamidation to glutamate (30). To determine whether this is also the case for a glutamine at Tsr residue 502, we compared the signal outputs and SDS-PAGE profiles of Tsr-EEEEQ and Tsr-EEEEE receptors in various host strains. In an R^- B^- strain (UU2610), Tsr-EEEEQ produced more CW flagellar rotation than did Tsr-EEEEE (Table S3), consistent with their different dose-response behaviors in FRET assays (Fig. 3A). If E502Q can be deamidated to glutamate by CheB, then the signal output of Tsr-EEEEQ in an R^- B^+ strain (UU2611) should approach that of Tsr-EEEEE. However, the flagellar rotation pattern produced by Tsr-EEEEQ showed no CheB-dependent change (Table S3), suggesting that physiological levels of CheB cannot appreciably deamidate E502Q. In support of this conclusion, Tsr-EEEEQ subunits expressed in the R^- B^+ strain also showed no CheB-dependent bandshifts upon SDS-PAGE analysis (Fig S2A). However, high-level expression of CheB from an inducible plasmid shifted Tsr-EEEEQ to the EEEEE state (Fig. 6A),

UU IR Author Manuscript

demonstrating that deamidation can occur at site 5, but less efficiently than it does at sites 1-4.

CheB-dependent demethylation at Tsr-E502. If CheB-dependent deamidation at E502Q occurs inefficiently, is CheB-mediated demethylation of methylated E502 (E502m) also inefficient? To answer this question, we expressed Tsr-NDNDE in an R^+ B^+ host (UU2612). At mid-exponential growth phase, the culture was treated with chloramphenicol to stop further protein synthesis and cell samples were taken at 15-minute intervals and analyzed by SDS-PAGE (Fig. S2). Under these conditions, any band shifts that occur must be due to modifications at residue E502 (see Fig. 5). At time zero, two Tsr bands were evident, corresponding to the unmethylated (NDNDE) and methylated (NDNDEm) forms of Tsr. With continued incubation in the absence of new protein synthesis, the unmethylated (NDNDE) form of Tsr became less prominent, indicating net conversion of Tsr to the methylated form (Fig. S2). Thus, at physiological levels of CheR and CheB, methylation at residue E502 is evident, but E502m demethylation is not.

As a more stringent test for whether E502m demethylation can occur, we expressed plasmid-encoded Tsr-NDNDE in an R^+ B^+ strain (UU2612) that also carried a compatible, salicylate-inducible CheB expression plasmid (pPA827). At mid-exponential growth stage, we induced CheB over-expression and followed Tsr modification state over a 60-minute timecourse by SDS-PAGE (Fig. 6B). In this experiment, the methylated band (E502m) diminished over time and the unmethylated band (E502) increased in intensity (Fig. 6B). The ratio of the two band intensities (E502m:E502) decreased linearly over the 60-minute timecourse in both the uninduced and induced cultures, but the rate of demethylation was faster in the induced culture (Fig. 6C). Thus, CheB-mediated demethylation occurs at site 5, but requires high levels of CheB to detect. The demethylation efficiency of E502m is evidently lower than it is for other Tsr adaptation sites.

UU IR Author Manuscript

Signaling effects of amino acid replacements at E502. The E502I and E502P mutant receptors were the only ones in the Tsr-E502* set that could not support serine chemotaxis in tryptone soft agar assays (Fig. 2). To explore the functional defect(s) caused by these particular amino acid replacements at E502, we examined the signaling properties of the mutant receptors with *in vivo* FRET kinase assays in host strains that had various combinations of the CheR and CheB adaptation enzymes (Fig. 7; Table S4). For comparison we also tested Tsr-E502Q, which mediated reduced-sensitivity serine chemotaxis in an adaptation-proficient host (Fig. 2). In an R^- B^- strain (UU2567) lacking both adaptation enzymes, Tsr-wt (QEQEE) produced a sensitive, highly cooperative response to serine ($K_{1/2}$ ~17 μM; Hill coefficient ~15), whereas the E502I, E502P, and E502Q receptors failed to respond even to 10 mM serine (Fig. 7; Table S4). In an R^+ B^+ strain (UU2700) containing both adaptation enzymes, Tsr-wt showed more sensitive, but less cooperative signaling behavior ($K_{1/2}$ ~0.4 μM; Hill coefficient ~2.4). All three mutant receptors also showed serine responses in the adaptation-proficient host, implying that they can undergo CheR and/or CheB modifications that improve their signaling properties. In that background Tsr-E502Q ($K_{1/2}$ ~8.6 μM) was somewhat less sensitive than Tsr-wt, consistent with its higher serine threshold in plate assays (Fig. 2) and an ON-biased signaling change. E502I was much less sensitive and more cooperative ($K_{1/2}$ ~133 μM; Hill coefficient ~5.4), whereas E502P showed nearly wild-type sensitivity and cooperativity (Fig. 7; Table S4).

To determine the nature of the output shifts caused by the E502I and E502P lesions, we examined their signaling responses in hosts containing only one of the two adaptation enzymes. CheR-mediated methylation should shift Tsr output to the ON state, thereby reducing response sensitivity to serine, whereas CheB-mediated deamidation and demethylation should shift output toward the OFF state to enhance serine sensitivity (see Fig. 3). Indeed, Tsr-wt had an elevated serine threshold in an R^+ B^- strain (UU2697) and failed to respond in an R^- B^+ strain (UU2699) (Fig. 7; Table S4), which probably deamidated the wild-type receptor molecules to the unresponsive

EEEEE state (see Table S1). Tsr-E502I produced a serine response in the R^- B^+ strain, but not in the R^+ B^- strain, consistent with an intrinsic ON-biased output (Fig. 7; Table S4). In contrast, CheR function alone restored E502P responsiveness, whereas CheB did not, suggesting that Tsr-E502P has an intrinsic OFF-biased output (Fig. 7; Table S4).

These tests also revealed some unexpected dose-response behaviors: (i) The E502Q receptor became more sensitive to serine in both the R^+ B^- and R^- B^+ strains. (ii) The E502Q and E502I receptors were most sensitive to serine in the host with both adaptation enzymes (Fig. 7; Table S4). (iii) The E502P receptor was more sensitive in the R^+ B^- host than it was in the R^+ B^+ host. We interpret these paradoxical behaviors as evidence for a direct influence of the CheR protein on receptor signaling complexes (31). Whereas CheB can enhance receptor sensitivity through its enzymatic activities (23, 31), CheR might promote attractant responses by preferentially binding to receptors in the OFF signaling state (31). This model predicts that the catalytic activity of CheR may play no role in shifting receptors to the OFF state, and may even compete with that signaling effect. Experiments that test these ideas will be the subject of a follow-up study.

DISCUSSION

HAMP signaling models. HAMP domains mediate input-output transactions in many bacterial signaling proteins. Two types of mechanistic models have been proposed for HAMP signaling. Two-state mechanisms, such as the gearbox model (32), postulate discrete, alternative HAMP conformations that elicit different output signals, for example, low versus high kinase activity. The proposed gearbox signaling states correspond to different packing arrangements of the four-helix HAMP bundle. In contrast, the dynamic bundle model proposes that overall HAMP packing stability, defined by ensembles of isoenergetic conformations, controls output activity (33).

HAMP function has been most intensively investigated in sensor histidine kinases and in MCP-family chemoreceptors. In the chemoreceptor models, a sensory adaptation system modulates HAMP operation, allowing for experimental manipulation of the structural interplay between HAMP and adjoining methylation sites. This study focused on Tsr-E502, a methylation site seemingly unique to the serine chemoreceptor of *E. coli*. Amino acid replacements at this Tsr residue produced a variety of mutant signaling behaviors that are most readily explained by the dynamic bundle model of HAMP output control (33).

Structural interplay of the HAMP and MH bundles. The dynamic-bundle model proposes that a four-residue phase stutter segment between the AS2 and MH1 helices couples the structural stabilities of the HAMP and MH bundles in opposition (Fig. 8A). Thus, optimal packing of the helices in the HAMP bundle forces the adjoining methylation site helices away from their optimal packing arrangement in the MH bundle, leading to kinase-off output. Conversely, tighter packing of the MH bundle destabilizes the HAMP bundle and produces kinase-on output. This model predicts that chemoeffector stimuli elicit signaling responses by influencing HAMP stability and that the sensory adaptation system terminates those responses by adjusting the opposed packing stability of the MH bundle: Methylation enhances stability; demethylation and deamidation reduce stability.

Extensive studies of methylation sites 1-4 in the aspartate receptor Tar, which are structurally analogous to Tsr sites 1-4, suggest that adaptational modifications regulate receptor output by controlling the packing stability of the four-helix methylation bundle (6, 7, 34). Unmethylated adaptation sites that contain negatively charged glutamic acid (E) residues could destabilize the MH bundle through localized electrostatic effects on helix structure and coiled-coil packing interactions. Methylation of E residues forms glutamyl methyl-esters (Em), which are uncharged and should enhance MH packing. Indeed, mutational replacement of a methyl-accepting E site with a variety of uncharged amino acids can mimic the signaling effects of methylation (Fig. 4; Table S2; Table S3)

UU IR Author Manuscript

(35-37). Glutamine (Q), which is closest in structure to a glutamyl methyl-ester, is the best methylation mimic, but less effective than methylation in its signaling effects (24).

Tsr methylation sites 1-4 lie at the subunit interface in receptor dimers (Fig. 1B; Fig. 8B) and should influence MH bundle stability most directly by modulating the strength of inter-subunit packing interactions. In contrast, Tsr-E502 lies close to the interface between N and C helices from the same subunit of the receptor dimer. Accordingly, we suggest that Tsr site 5 influences overall MH bundle stability by modulating the strength of intra-subunit packing interactions (Fig. 8B).

Signaling consequences of adaptational modifications at Tsr-E502. Tsr-E502 undergoes CheR-mediated methylation (Fig. 5) (8) and, less efficiently, CheB-dependent demethylation (Fig. 6B and 6C). Using Q residues as a proxy for methylated E sites in hosts lacking CheR function, we found that Tsr-EEEEQ receptors produced high levels of CW rotation, whereas Tsr-EEEEE did not (Table S3). Moreover, Tsr-EEEEE did not generate enough kinase activity to detect a signaling response to serine, whereas Tsr-EEEEQ responded well, but with a substantially higher threshold than wild-type (QEQEE) Tsr (Table S1). Other single-Q Tsr variants (*e.g.*, QEEEE) detected serine with thresholds lower than that of wild-type Tsr (Table S1).

Although a Q at residue 502 shifts Tsr output toward the kinase-on state, as do Q residues at Tsr adaptation sites 1-4, the E502Q receptor exhibited a very large increase in serine detection threshold (Table S1). We ascribe the signaling potency of Tsr-E502 to two structural factors: (i) the unique ability of this modification site to modulate intra-subunit, rather than inter-subunit, packing stability of the MH bundle (Fig. 8B); and (ii) the close proximity of Tsr site 5 to the AS2 output helices of HAMP (Fig. 8A). Although Tsr-E502 does not have a direct covalent connection to the AS2 helix, the dynamic bundle model predicts that methylation at site 5 could exert a strong destabilizing effect on the HAMP bundle through its stabilizing effects on MH bundle packing. Conceivably, the intensity of the structural clash between the HAMP and MH bundles declines with distance from the phase stutter connection.

UU IR Author Manuscript

Signaling consequences of amino acid replacements at Tsr-E502. The wild-type E502 residue of Tsr is likely to have a destabilizing effect on local MH bundle packing near the HAMP junction (Fig. 8C). In the modeled bundle structure, extrapolated from the X-ray structure of the Tsr hairpin tip (38), the negatively charged side chain of E502 resides in a moderately hydrophobic cavity lined with alanine residues from both the C and N helices in each subunit. In addition, Y278 from the N helix caps the cavity (Fig. 8C). Although the polar E502 carboxyl group might H-bond to the tyrosine hydroxyl group, this interaction alone is unlikely to stabilize the E side-chain in the cavity. We suggest that E502 is a good substrate for CheR-mediated methylation because its acidic side chain adopts a less buried, more exposed location. Additionally, looser packing of the MH helices in the vicinity of E502 might promote CheR recognition and docking.

Neutralization of the E502 carboxyl group through CheR-mediated methylation should enhance intra-subunit packing forces and make the Em side chain less solvent-accessible. A more buried side chain would explain why receptors methylated at E502 are not readily demethylated by CheB (Fig. 6B and 6C). Similar reasoning applies to Tsr-E502Q, which is a poor substrate for CheB-mediated deamidation (Fig. 6A; Fig. S2). In the context of the dynamic bundle model, tighter packing of the MH bundle would also make it more difficult for serine binding to drive HAMP to its stable, kinase-off, signaling state (Fig. 8A), thus accounting for the high response threshold of the Tsr-E502Q receptor (Fig. 7).

Only two amino acid replacements at E502 fully abrogated Tsr function. Tsr-E502P exhibited signaling properties consistent with a large shift to the kinase-off output state. CheR function (*i.e.*, conversion of E to Em) shifted the mutant receptors to a serine-responsive condition, whereas CheB function alone did not (Fig. 7). In contrast, Tsr-E502I exhibited signaling properties characteristic of a large shift to the kinase-on output state. CheB function (*i.e.*, conversion of Q to E) shifted Tsr-E502I to a responsive range, whereas CheR function alone did not (Fig. 7).

The signaling behavior of Tsr-E502P probably reflects local destabilization of the proline-containing helix and a consequent drop in MH bundle packing stability, comparable to that of an unmethylated receptor, which generates little kinase activity (*e.g.*, Tsr-EEEEE; Table S1; Table S3). An isoleucine side chain at residue 502 might, instead, prefer the hydrophobic environment of the 502 cavity, thereby enhancing intra-subunit and MH bundle packing interactions, perhaps approximating the structural stability of highly modified receptors (*e.g.*, Tsr-QQQQQ), whose kinase activity cannot be down-regulated (Table S1; Table S3).

Structural insights from SDS-PAGE bandshifts. Every amino acid replacement at residue E502 shifted Tsr subunit mobility in denaturing gel electrophoresis (Fig. 2; Fig. S1). Perhaps receptor subunits retain some native secondary and tertiary structures in the presence of SDS. If so, then interactions between those structural elements could influence gel migration rates. For example, pairing interactions between the N and C helices that are subject to E502 control in native Tsr might accelerate subunit migration, whereas extended, non-interacting helices might cause slower gel mobility. This interpretation is consistent with the proposed structural consequences of amino acid replacements at E502: P (and the wild-type E) most likely reduce intra-subunit and MH bundle packing interactions, whereas Q and I probably enhance those interactions. E502P subunits had the slowest SDS-PAGE mobility; E502I had the fastest (Fig. 2; Fig. S1). Conceivably, the relative mobilities of other mutant subunits reflect similar structural and signaling changes.

Chemotactic signaling role of Tsr-E502. The fifth methylation site of Tsr is not critical for chemotaxis because most mutant receptors with an E502 amino acid replacement mediated normal chemotactic behavior on tryptone soft agar (Fig. 2). A few changes (K, Q, G, D, M) caused demonstrably reduced detection sensitivity, but even so, the remaining sensory adaption sites compensated effectively for the on-shifted outputs of these mutant receptors.

UU IR Author Manuscript

Tsr residue E502 is also not sufficient for chemotaxis: It failed to support Tsr function when adaptation sites 1-4 were rendered nonfunctional. The disparity in CheR and CheB modification rates at site 5 probably contributes to this functional deficit. CheR-mediated methylation occurs more readily at E502 than does CheB-mediated deamidation or demethylation. Considering the small number of CheB molecules that operate in a normal receptor array (39), methylation at E502 might be effectively irreversible. Perhaps methylation of Tsr-E502 is an adaptational modification of last resort that only comes into play at very high serine levels. Perhaps other *E. coli* MCPs lack a corresponding adaptation site because the cells seldom encounter, or prefer to ignore, high levels of their cognate ligands.

In summary, our study of Tsr-E502 has provided new insights into how the structural interplay between HAMP and adjoining sensory adaptation elements controls the signaling behavior of a chemoreceptor.

ACKNOWLEDGEMENTS

This work was supported by research grant GM19559 from the National Institute of General Medical Sciences. We thank Germán Piñas (U. Utah) and Runzhi Lai (U. Utah) for comments on the manuscript and Sung-Hou Kim (UC-Berkeley) for Tsr atomic coordinates. The Protein-DNA Core Facility at the University of Utah receives support from National Cancer Institute grant CA42014 to the Huntsman Cancer Institute.

REFERENCES

1. **Hazelbauer GL, Falke JJ, Parkinson JS.** 2008. Bacterial chemoreceptors: high-performance signaling in networked arrays. Trends. Biochem. Sci. **33:**9-19.

2. **Sourjik V, Armitage JP.** 2010. Spatial organization in bacterial chemotaxis. EMBO J. **29:**2724-2733.

3. **Porter SL, Wadhams GH, Armitage JP.** 2011. Signal processing in complex chemotaxis pathways. Nature reviews. Microbiology **9:**153-165.

4. **Terwilliger TC, Wang JY, Koshland DE, Jr.** 1986. Surface structure recognized for covalent modification of the aspartate receptor in chemotaxis. Proc. Natl. Acad. Sci. USA **83:**6707-6710.

5. **Nowlin DM, Bollinger J, Hazelbauer GL.** 1987. Sites of covalent modification in Trg, a sensory transducer of Escherichia coli. J. Biol. Chem. **262:**6039-6045.

6. **Starrett DJ, Falke JJ.** 2005. Adaptation mechanism of the aspartate receptor: electrostatics of the adaptation subdomain play a key role in modulating kinase activity. Biochemistry **44:**1550-1560.

7. **Winston SE, Mehan R, Falke JJ.** 2005. Evidence that the adaptation region of the aspartate receptor is a dynamic four-helix bundle: cysteine and disulfide scanning studies. Biochemistry **44:**12655-12666.

8. **Rice MS, Dahlquist FW.** 1991. Sites of deamidation and methylation in Tsr, a bacterial chemotaxis sensory transducer. J. Biol. Chem. **266:**9746-9753.

9. **Parkinson JS.** 2010. Signaling mechanisms of HAMP domains in chemoreceptors and sensor kinases. Annu. Rev. Microbiol. **64:**101-122.

10. **Parkinson JS, Houts SE.** 1982. Isolation and behavior of *Escherichia coli* deletion mutants lacking chemotaxis functions. J. Bacteriol. **151:**106-113.

11. **Ames P, Studdert CA, Reiser RH, Parkinson JS.** 2002. Collaborative signaling by mixed chemoreceptor teams in *Escherichia coli*. Proc. Natl. Acad. Sci. USA **99:**7060-7065.

12. **Zhou Q, Ames P, Parkinson JS.** 2011. Biphasic control logic of HAMP domain signalling in the *Escherichia coli* serine chemoreceptor. Mol. Microbiol. **80:**596-611.

13. **Chang ACY, Cohen SN.** 1978. Construction and characterization of amplifiable multicopy DNA cloning vehicles derived from the p15A cryptic miniplasmid. J. Bacteriol. **134:**1141-1156.

14. **Gosink KK, Buron-Barral M, Parkinson JS.** 2006. Signaling interactions between the aerotaxis transducer Aer and heterologous chemoreceptors in *Escherichia coli*. J. Bacteriol. **188:**3487-3493.

15. **Bolivar F, Rodriguez R, Greene PJ, Betlach MC, Heyneker HL, Boyer HW.** 1977. Construction and characterization of new cloning vehicles. Gene **2:**95-113.

16. **Studdert CA, Parkinson JS.** 2005. Insights into the organization and dynamics of bacterial chemoreceptor clusters through *in vivo* crosslinking studies. Proc. Natl. Acad. Sci. USA **102:**15623-15628.

17. **Sourjik V, Vaknin A, Shimizu TS, Berg HC.** 2007. In vivo measurement by FRET of pathway activity in bacterial chemotaxis. Methods Enzymol **423:**363-391.

18. **Parkinson JS.** 1976. *cheA*, *cheB*, and *cheC* genes of *Escherichia coli* and their role in chemotaxis. J. Bacteriol. **126:**758-770.

19. **Laemmli UK.** 1970. Cleavage of structural proteins during assembly of the head of bacteriophage T4. Nature **227:**680-685.

20. **Ames P, Parkinson JS.** 1994. Constitutively signaling fragments of Tsr, the *Escherichia coli* serine chemoreceptor. J. Bacteriol. **176:**6340-6348.

21. **Slocum MK, Parkinson JS.** 1985. Genetics of methyl-accepting chemotaxis proteins in *Escherichia coli*: null phenotypes of the *tar* and *tap* genes. J. Bacteriol. **163:**586-594.

22. **Berg HC, Block SM.** 1984. A miniature flow cell designed for rapid exchange of media under high-power microscope objectives. J. Gen. Microbiol. **130:**2915-2920.

23. **Sourjik V, Berg HC.** 2002. Receptor sensitivity in bacterial chemotaxis. Proc. Natl. Acad. Sci. USA **99:**123-127.

24. **Shimizu TS, Tu Y, Berg HC.** 2010. A modular gradient-sensing network for chemotaxis in Escherichia coli revealed by responses to time-varying stimuli. Mol. Syst. Biol. **6:**382.

25. **Sourjik V, Berg HC.** 2004. Functional interactions between receptors in bacterial chemotaxis. Nature **428:**437-441.

26. **BD Bionutrients Technical Manual**, Third Edition Revised, 2006.

27. **Bornhorst JA, Falke JJ.** 2001. Evidence that both ligand binding and covalent adaptation drive a two- state equilibrium in the aspartate receptor signaling complex. J. Gen. Physiol. **118:**693-710.

28. **Li G, Weis RM.** 2000. Covalent modification regulates ligand binding to receptor complexes in the chemosensory system of *Escherichia coli*. Cell **100:**357-365.

29. **Shapiro MJ, Koshland DE, Jr.** 1994. Mutagenic studies of the interaction between the aspartate receptor and methyltransferase from *Escherichia coli*. J. Biol. Chem. **269:**11054-11059.

30. **Kehry MR, Bond MW, Hunkapiller MW, Dahlquist FW.** 1983. Enzymatic deamidation of methyl-accepting chemotaxis proteins in *Escherichia coli* catalyzed by the *cheB* gene product. Proc. Natl. Acad. Sci. USA **80:**3599-3603.

31. **Kim C, Jackson M, Lux R, Khan S.** 2001. Determinants of chemotactic signal amplification in *Escherichia coli*. J. Mol. Biol. **307:**119-135.

32. **Hulko M, Berndt F, Gruber M, Linder JU, Truffault V, Schultz A, Martin J, Schultz JE, Lupas AN, Coles M.** 2006. The HAMP domain structure implies helix rotation in transmembrane signaling. Cell **126:**929-940.

33. **Zhou Q, Ames P, Parkinson JS.** 2009. Mutational analyses of HAMP helices suggest a dynamic bundle model of input-output signalling in chemoreceptors. Mol. Microbiol. **73:**801-814.

34. **Swain KE, Gonzalez MA, Falke JJ.** 2009. Engineered socket study of signaling through a four-helix bundle: evidence for a yin-yang mechanism in the kinase control module of the aspartate receptor. Biochemistry **48:**9266-9277.

35. **Shapiro MJ, Chakrabarti I, Koshland DE, Jr.** 1995. Contributions made by individual methylation sites of the *Escherichia coli* aspartate receptor to chemotactic behavior. Proc. Natl. Acad. Sci. USA **92:**1053-1056.

36. **Nowlin DM, Bollinger J, Hazelbauer GL.** 1988. Site-directed mutations altering methyl-accepting residues of a sensory transducer protein. Proteins **3:**102-112.

37. **Nishiyama S, Nara T, Homma M, Imae Y, Kawagishi I.** 1997. Thermosensing properties of mutant aspartate chemoreceptors with methyl-accepting sites replaced singly or multiply by alanine. J. Bacteriol. **179:**6573-6580.

38. **Kim KK, Yokota H, Kim SH.** 1999. Four-helical-bundle structure of the cytoplasmic domain of a serine chemotaxis receptor. Nature **400:**787-792.

39. **Li M, Hazelbauer GL.** 2004. Cellular stoichiometry of the components of the chemotaxis signaling complex. J. Bacteriol. **186:**3687-3694.

FIGURE LEGENDS

Fig. 1. Structural features of Tsr and its methylation sites.

A. The Tsr homodimer. Cylindrical segments represent α-helices, drawn approximately to scale. Each Tsr subunit has five methylation sites (bolded residues in the primary sequence: sites 1-4 are in white; site 5 is in black.

B. Structure of the native methylation helix (MH) bundle. Shown are residues R271-A320 and A462-V512 in each subunit of the Tsr dimer. One subunit is shaded gray, the other dark gray. Methylation sites 1-4 (white atoms) lie near the inter-subunit interface; methylation site 5 (black atoms) lies near the intra-subunit interface. The atomic coordinates were modeled and extrapolated from the crystal structure of the kinase control region of Tsr (38).

Fig. 2. Mutational survey of Tsr-E502. Bold letters below the histogram indicate the amino acid at residue 502 of Tsr (E = Tsr wild-type). White and black bars indicate the relative colony size on tryptone soft agar produced by strain UU1250 carrying a plasmid expressing each Tsr variant. White bars denote wild-type colony morphology; black bars denote colonies with no evident ring of chemotactic cells at their periphery. Gray bars indicate the relative expression levels of the mutant Tsr proteins. Black horizontal bars beneath the mutant amino acid indicate the relative positions of the mutant subunits in SDS-PAGE analyses (see Fig. S1). Dashed horizontal gray lines are simply intended to facilitate comparison of band positions. Serine thresholds of the Tsr-E502 mutants were defined by chemotactic ring formation on minimal soft agar plates containing 2.5, 20, or 100 μM serine. Amino acid replacement mutants are arranged left to right within each threshold group in order of decreasing colony size on tryptone soft agar.

Fig. 3. Dose-response behaviors of Tsr-Q/E variants. Plasmid pRR53 and pPA114 derivatives encoding Tsr variants with different combinations of E and Q residues at methylation sites 1-5 were tested for serine responses in strain

UU2567 (R^- B^-) carrying the pRZ30 or pVS88 FRET reporter plasmid, respectively.

A. Hill fits for three Tsr-Q/E variants. Individual fits were done to aggregate data from several independent experiments (see Table S1) to illustrate the extent of variability in the FRET-derived data. $K_{1/2}$, Hill coefficient, and number of experiments were: Tsr-QEEEE (5.1 μM; 8.9; 2); Tsr-QEQEE (16.9 μM; 8.3; 4); Tsr-EEEEQ (90 μM;11.7; 2).

B. Summary of average $K_{1/2}$ values for all Tsr-Q/E variants tested (see Table S1). Tsr variants with E at site 5 (○); Tsr variants with Q at site 5 (◇). Receptors with ln $K_{1/2}$ values >9 showed no kinase inhibition response to a 10 mM serine stimulus.

Fig. 4. Dose-response behaviors of Tsr-N/D variants. Plasmid pRR53 derivatives encoding Tsr variants with different combinations of D and N residues at methylation sites 1-4 were tested for serine responses in strain UU2567 (R^- B^-) carrying the pRZ30 FRET reporter plasmid. Solid line fits were to unaveraged data from one or more independent experiments (Table S2). The fit for Tsr-wt (QEQEE; dashed line) was obtained by averaging data points from four independent experiments (Fig. 3A and Table S1). $K_{1/2}$ and Hill coefficient values in these experiments were: Tsr-DDDDE (3.1 μM; 7.9); Tsr-NDDDE (6.5 μM; 6.0); Tsr-NDNDE (50 μM; 11.3); Tsr-QEQEE (16.2 μM; 10.2).

Fig. 5. Methylation of Tsr residue E502. Panels show SDS-PAGE migration patterns of Tsr subunits (see Methods). Triplet bands are modification variant standards; from slowest to fastest: Tsr-EEEEE; Tsr-QEQEE (wild type); Tsr-QQQQE.

A. Band profiles of Tsr variants in host strains expressing different combinations of the CheR and CheB enzymes: R^- B^- (UU2610); R^- B^+ (UU2611); R^+ B^- (UU2632); R^+ B^+ (UU2612). In Tsr-DDDDE and Tsr-NDNDE, only E502 is available for methylation, whereas in wild-type Tsr (QEQEE),

multiple sites are available for deamidation, methylation, and demethylation.

B. CheR-dependent band shift of Tsr-NDNDE compared to Tsr-NDNDD.

Fig. 6. Deamidation and demethylation at Tsr residue 502.

A. SDS-PAGE profile of Tsr-EEEEQ subunits expressed from pRR53 in strain UU2611 (R^- B^+) carrying a salicylate-inducible CheB expression plasmid (pPA827): - (no salicylate induction); + (2 μM salicylate).

B. Demethylation timecourse of Tsr-NDNDE expressed from pRR53 in strain UU2612 (R^+ B^+) carrying plasmid pPA827: - (no salicylate induction); + (2 μM salicylate). Protein samples taken at 30-minute intervals after addition of the CheB inducer were analyzed by SDS-PAGE.

C. Quantitation of demethylation timecourse in panel B. The relative intensities of methylated (E502m) and unmethylated (E502) Tsr subunits were determined by area integration of the corresponding gel bands using ImageJ software.

Fig. 7. Dose-response behaviors of Tsr-E502Q, Tsr-E502I, and Tsr-E502P.

Plasmid pPA114 derivatives encoding Tsr-E502 mutant proteins were tested for serine responses in four different hosts carrying the pVS88 FRET reporter plasmid: UU2567 (R^- B^-, ◇); UU2700 (R^+ B^+, ◆); UU2697 (R^+ B^-,▲); UU2699 (R^- B^+,▼). Note that the UU2697 and UU2699 data can be less precise because sub-saturating stimuli may elicit Tsr modification state changes (methylation in UU2697; deamidation in UU2699) that affect subsequent responses. Solid lines indicate Hill fits to data from one or more independent experiments (Table S4). Dashed lines indicate the Hill fit to Tsr-wt (QEQEE) data averaged from two independent experiments (Table S4).

Fig. 8. Mechanistic interpretation of Tsr-E502 signaling effects.

A. Dynamic-bundle model of HAMP domain signal control in Tsr **(33)**. The phase stutter connection at the HAMP-MH bundle junction is proposed to produce an oppositional stability relationship between packing of the HAMP and MH bundles. Open arrows between the bundles indicate the direction of

UU IR Author Manuscript

structure-destabilizing forces: Tight packing of HAMP (horizontal black lines) destabilizes MH bundle packing (light gray lines), leading (by an unspecified mechanism) to deactivation of CheA. A second kinase-OFF state (not shown because it did not arise in the experiments of this study) results when MH packing is tight and HAMP packing is loose (9). CheA activation occurs (by an unspecified mechanism) when the MH and HAMP bundles have intermediate packing stabilities (dark gray lines). Attractants and repellents produce stimulus responses by acting on HAMP stability; subsequent methylation (sites 1-4 [gray]; site 5 [black]) and demethylation (sites 1-5 [white]) changes produce sensory adaptation by shifting the packing stability of the MH bundle to counterbalance HAMP input effects, driving the system back to an intermediate set-point stability.

B. Proposed structure-stabilizing effects of receptor methylation. The four helices of the MH bundle are shown in cross-section, as viewed from the membrane toward the cytoplasmic tip. Adaptation sites 1-4 (gray) probably modulate MH bundle stability by influencing inter-subunit interactions (gray arrows); site 5 (black) probably modulates MH bundle stability by influencing intra-subunit interactions (black arrows). Unmethylated, negatively charged E residues should lower MH bundle stability; methylation (or uncharged amino acid replacements, such as Q), should stabilize MH bundle packing interactions.

C. Local structural environment of Tsr-E502. Segments of the MH1 (N275-T286) and MH2 (A495-S506) helices from one subunit of the Tsr dimer are shown. All C, N, and O atoms are shown as spheres, except for E502, whose main-chain atoms are not shown and whose side-chain is shown as black sticks and space-filling dots. Hydrophobic amino acids whose side chain is within 5Å of E502 side-chain atoms are shown in white; other residues are gray. The Y278 label line points to the oxygen atom of the side-chain hydroxyl group on

UU IR Author Manuscript

the aromatic ring. Label lines for A281, A285, A498, and A499 point to the carbon atom of their side chain methyl group.

UU IR Author Manuscript

Fig. 1.

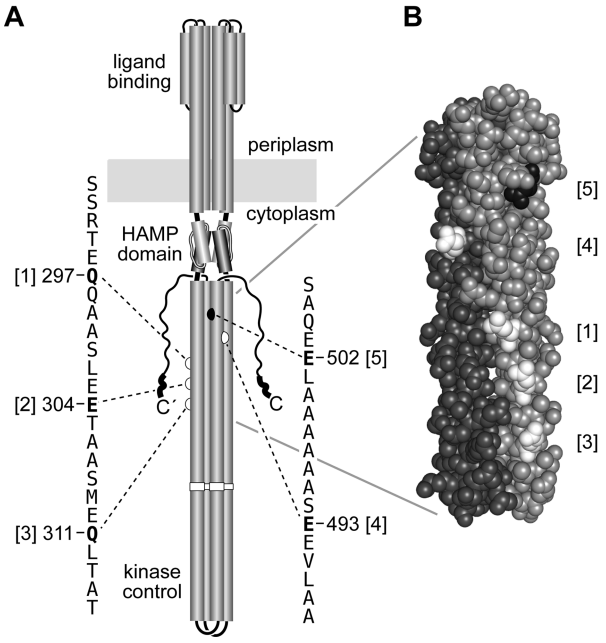

Fig. 2.

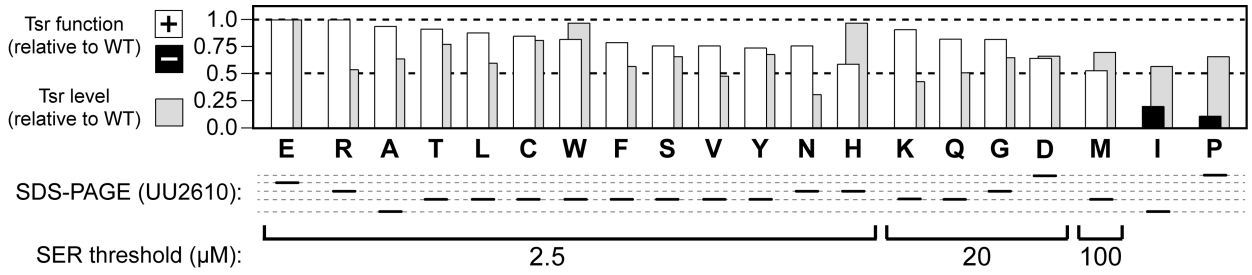

UU IR Author Manuscript

Fig. 3.

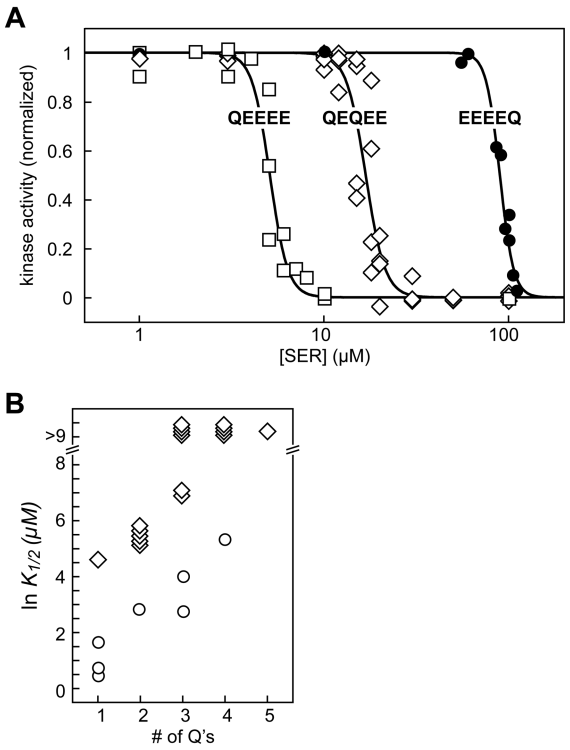

UU IR Author Manuscript

Fig. 4.

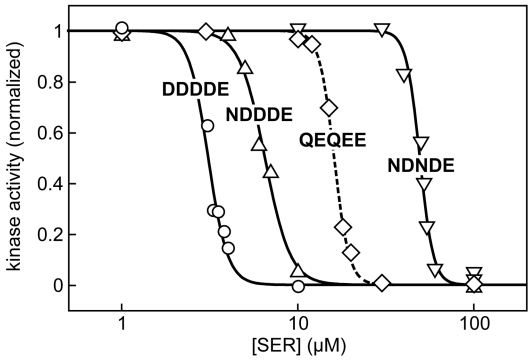

Fig. 5.

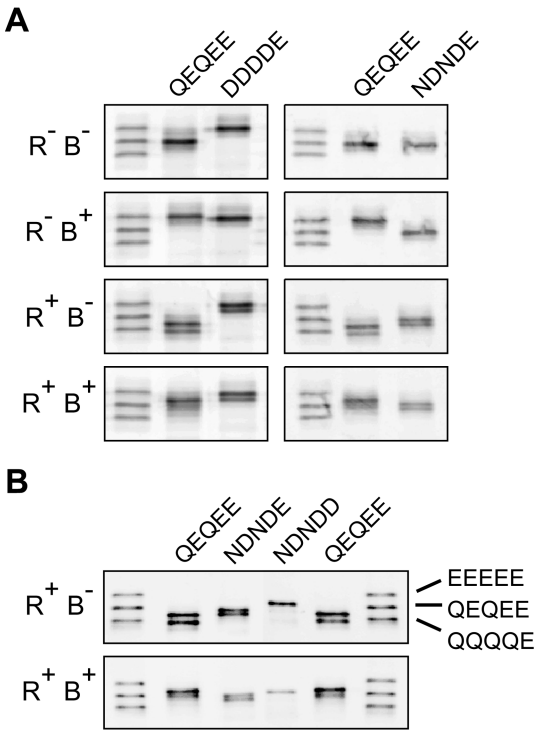

UU IR Author Manuscript

Fig. 6.

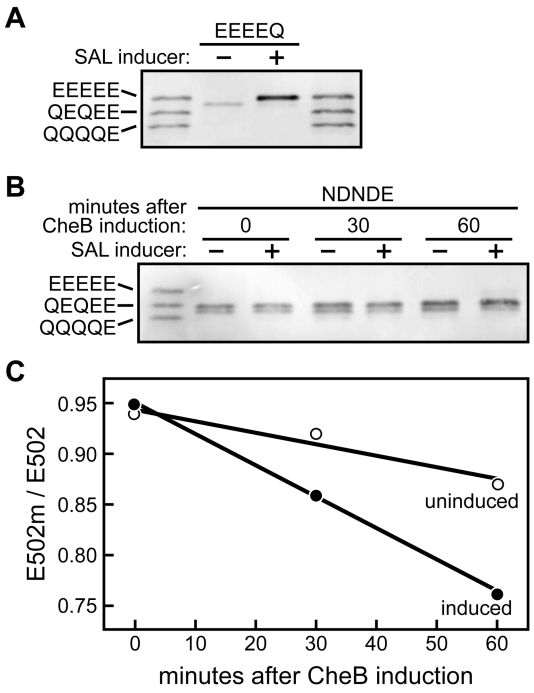

UU IR Author Manuscript

Fig. 7.

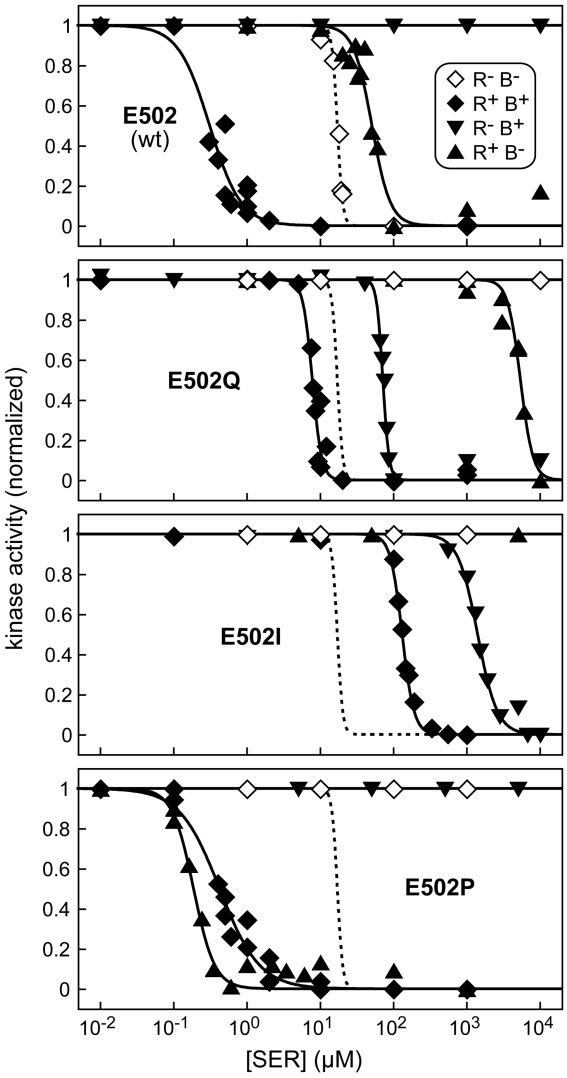

Fig. 8.

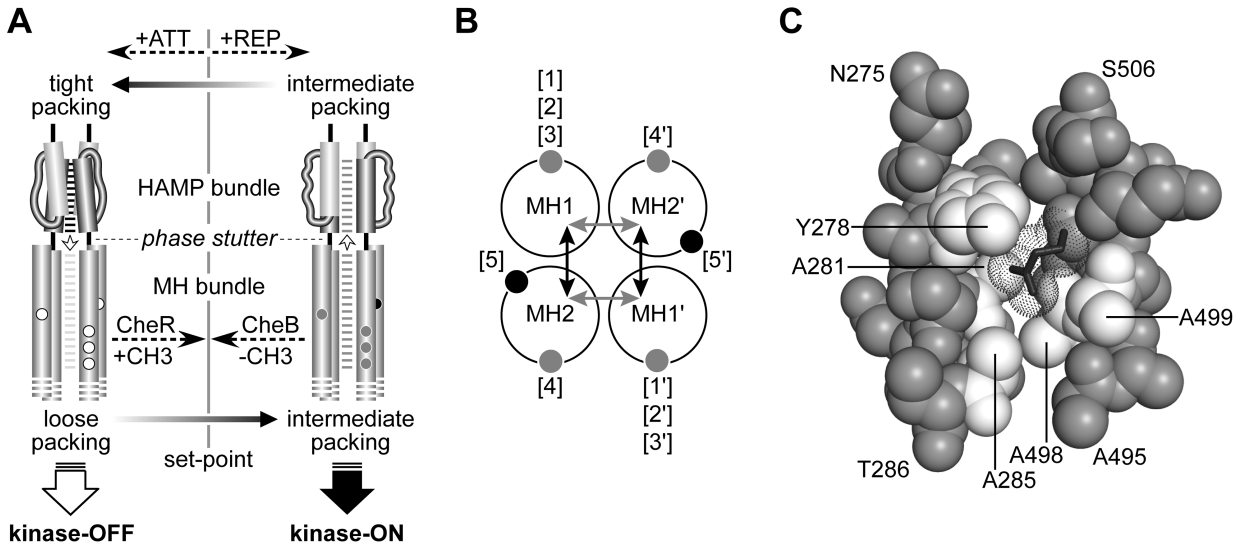

UU IR Author Manuscript

Table S1. Serine dose-response parameters for Tsr-Q/E variants in strain UU2567.

# Q's	modification site residues	receptor & FRET reporter plasmids	$K_{1/2}$ (μM) [a]	Hill coefficient [a]	number of experiments
E at fifth site:					
0	E E E E E	pRR53 & pRZ30	NR	NR	5
1	E E Q E E	pRR53 & pRZ30	2.2 ± 0.5	5.5 ± 1.0	5
1	E E E Q E	pRR53 & pRZ30	1.9 ± 0.7	3.7 ± 0.3	3
1	Q E E E E	pRR53 & pRZ30	5.3 ± 0.4	27 ± 3.7	3
2 (wt)	**Q E Q E E**	**pRR53 & pRZ30**	**17 ± 1.2**	**18 ± 5.0**	**4**
2 (wt)	**Q E Q E E**	**pPA114 & pVS88**	**17 ± 1.1**	**15 ± 7.5**	**2**
3	Q E Q Q E	pRR53 & pRZ30	15 ± 2.4	16 ± 6.7	3
3	Q Q Q E E	pRR53 & pRZ30	53 ± 1.5	14 ± 3.5	2
4	Q Q Q Q E	pRR53 & pRZ30	203 ± 7.0	8.5 ± 2.5	2
Q at fifth site:					
1	E E E E Q	pRR53 & pRZ30	104 ± 14	8.0 ± 4.0	2
2	E E E Q Q	pRR53 & pRZ30	202	7	1
2	E E E Q Q	pPA114 & pVS88	232 ± 52	14 ± 4.0	2
2	E Q E E Q	pPA114 & pVS88	216	16.0	1
2	Q E E E Q	pPA114 & pVS88	235	7.2	1
2	E E Q E Q	pPA114 & pVS88	284	16	1
3	E Q Q E Q	pPA114 & pVS88	1030	16	1
3	E E Q Q Q	pPA114 & pVS88	1138 ± 180	7.0 ± 1.0	2
3	E Q E Q Q	pPA114 & pVS88	NR	NR	1
3	Q E Q E Q	pPA114 & pVS88	NR	NR	1
3	Q Q E E Q	pPA114 & pVS88	NR	NR	1
3	Q E E Q Q	pPA114 & pVS88	NR	NR	1
4	E Q Q Q Q	pPA114 & pVS88	NR	NR	1
4	Q Q Q E Q	pPA114 & pVS88	NR	NR	1
4	Q E Q Q Q	pPA114 & pVS88	NR	NR	1
4	Q Q E Q Q	pPA114 & pVS88	NR	NR	1
5	Q Q Q Q Q	pRR53 & pRZ30	NR	NR	7

[a] For multiple experiments, means and standard errors were determined from the best-fit parameter values for each independent experiment. NR: no response to 10 mM serine.

Table S2. Serine dose-response parameters for Tsr-N/D variants in strain UU2567.

modification site residues	$K_{1/2}$ (μM) [a]	Hill coefficient [a]	number of experiments
D D D D E	3.5 ± 0.4	6.4 ± 1.5	2
N D D D E	6.5	6.0	1
D N D D E	5.2 ± 0.5	14 ± 1.9	2
N D N D E	43 ± 7.1	8.9 ± 2.3	2
N D N D D	NR	NR	4

Tsr variants were expressed from plasmid pRR53 derivatives in strain UU2567 containing the pRZ30 FRET reporter plasmid.

[a] For multiple experiments, means and standard errors were determined from the best-fit parameter values for each independent experiment. NR: no response to 10 mM serine.

UU IR Author Manuscript

Table S3. Flagellar rotation patterns produced by Tsr-Q/E and Tsr-N/D variants.

modification site residues [a]	%CW rotation time in UU2610	%CW rotation time in UU2611	%CW rotation time in UU2632	%CW rotation time in UU2612
E E E E E	18 ± 3 [2]	20 ± 0.5 [2]	nd	28
E E E E Q	72 ± 10 [2]	65 ± 5 [2]	nd	nd
Q Q Q Q E	61 ± 3 [3]	58 ± 8 [3]	57 ± 8 [3]	52 ± 16 [2]
Q Q Q Q Q	62 ± 3 [4]	61 ± 2 [2]	68 ± 13 [2]	87 ± 8 [2]
Q E Q E E (wt)	**68 ± 3 [5]**	**40 ± 9 [3]**	**70**	**25 ± 2 [3]**
D D D D E	70 ± 10 [2]	65	48 ± 9 [3]	32
N D D D E	69	61	48	46
D N D D E	63	66	47	70
N D N D E	59 ± 9 [3]	77	31 ± 8 [3]	77
N D N D D	62	48	48	49

[a] Derivatives of plasmid pRR53 were transferred to rotation host strains; induction with 50 μM IPTG.

Table S4. Serine dose-response parameters for Tsr-E502Q, Tsr-E502I, and Tsr-E502P.

Tsr mutant [a]	FRET host strain [b]	$K_{1/2}$ (μM) [c]	Hill coefficient [c]	number of experiments
wild-type				
	UU2567	17 ± 1.1	15 ± 7.5	2
	UU2699	NR	NR	1
	UU2697	49 ± 6.6	8.5 ± 4.8	3
	UU2700	0.4 ± 0.1	2.4 ± 0.2	2
E502Q				
	UU2567	NR	NR	2
	UU2699	73	10	1
	UU2697	5243 ± 100	13 ± 9.3	2
	UU2700	8.6 ± 0.75	9.2 ± 2.8	2
E502I				
	UU2567	NR	NR	5
	UU2699	1424	3	1
	UU2697	NR	NR	2
	UU2700	133	5.4	1
E502P				
	UU2567	NR	NR	5
	UU2699	NR	NR	2
	UU2697	0.2	3.0	1
	UU2700	0.5 ± 0.1	1.6 ± 0.05	2

[a] Derivatives of plasmid pPA114 were transferred to FRET host strains; induction with 0.6 μM sodium salicylate.

[b] Strains also carried the FRET reporter pVS88; induction with 50 μM IPTG.

[c] For multiple experiments, means and standard errors were determined from the best-fit parameter values for each independent experiment. NR: no response to 10 mM serine.

UU IR Author Manuscript

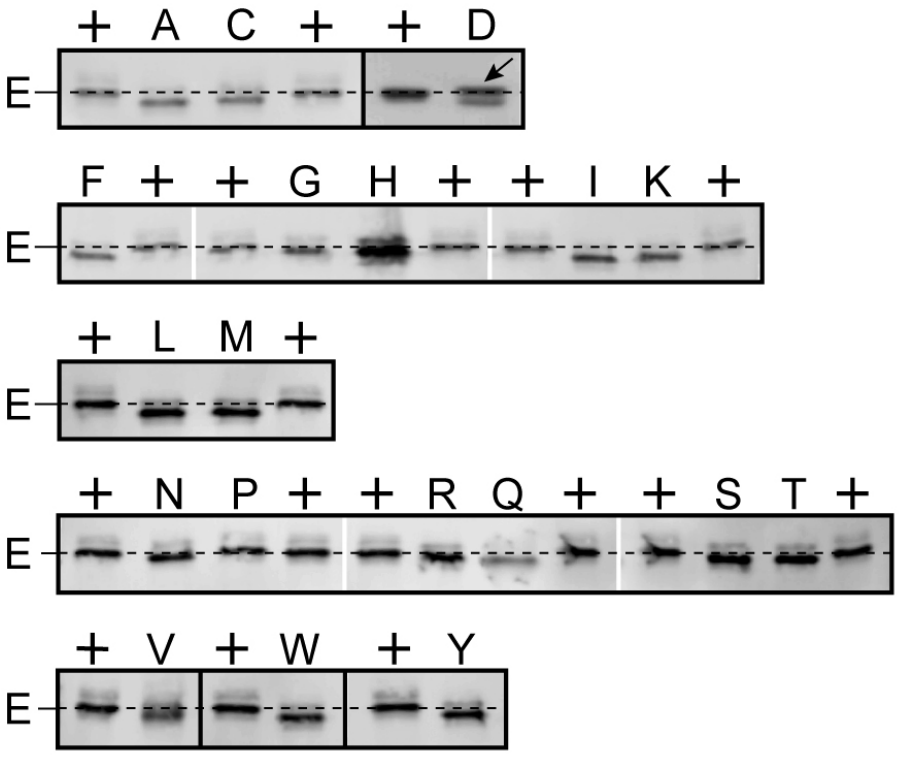

Fig. S1. Mobility of Tsr-E502* proteins in SDS-PAGE

Plasmid pPA114 Tsr-E502* derivatives were expressed in host strain UU2610, as detailed in Methods. Cell extracts were subjected to electrophoresis in denaturing 11% polyacrylamide gels and Tsr bands were visualized by immunoblotting. Lanes labeled + contain wild-type Tsr; letters above lanes indicate Tsr-E502 amino acid replacement proteins. Dashed horizontal lines indicate the positions of the wild-type bands (E) in each gel segment. Segments from the same gel that were individually adjusted to align the wild-type markers are separated by white vertical lines. Note that the wild-type lanes immediately adjacent to the white separators are the same. Individually ajusted segments of different gels or noncontiguous segments of the same gel are separated by a black vertical line. Samples of the Tsr-E502D protein contained variable amounts of a Tsr proteolysis product just below the uncleaved upper band (indicated with an arrow).

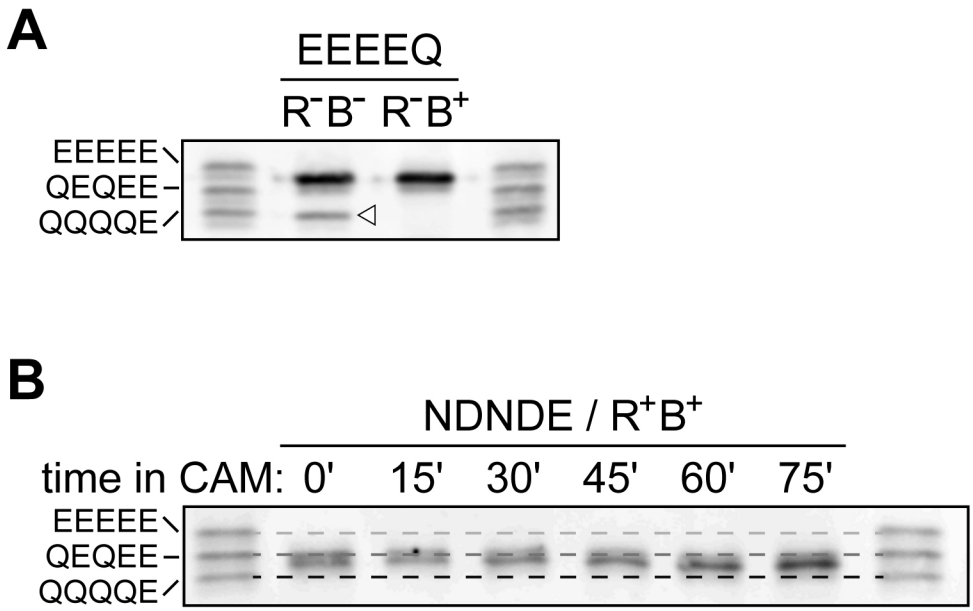

Fig. S2. Inefficient deamidation and demethylation at Tsr adaptation site 5 under physiological conditions.

A. Comparison of SDS-PAGE band profiles of Tsr-EEEEQ subunits produced in strain UU2610 (R^- B^-) and in strain UU2611 (R^- B^+). The minor band indicated with an open triangle is a Tsr proteolytic product that arises in some cell extracts.

B. Timecourse of methylation at Tsr-E502. Tsr-NDNDE was expressed in strain UU2612 (R^+ B^+). At time zero, chloramphenicol (CAM) was added to the culture to block further protein synthesis and samples were removed at the indicated times for SDS-PAGE analysis.